Available online at www.sciencedirect.com

ScienceDirect

Procedia Structural Integrity 40 (2022) 129–135

Structural Integrity Procedia

www.elsevier.com/locate/procedia

15th International Conference on Mechanics, Resource and Diagnostics of Materials and Structures

Lüders deformation in specimens made of normalized 09G2S steel

Farber V.M.[a], Morozova A. N.[b] *, Khotinov V.A.[a], Vichuzhanin D.I.[c], Karabanalov M.S.[a], Veretennikova I.A[c].

[a]*B. N. Yeltsin Ural Federal University, 19 Mira St., Ekaterinburg, 620002, Russia*
[b]*M. N. Miheev Institute of Metal Physics, Ural Branch of the Russian Academy of Sciences, 18 S. Kovalevskoy St., Ekaterinburg, 620108, Russia*
[c]*Institute of Engineering Science, Ural Branch of the Russian Academy of Sciences, 34 Komsomolskaya St., Ekaterinburg, 620049, Russia*

Abstract

The features of Lüders deformation in the normalized 09G2S steel are studied by the methods of digital image correlation, topography, and scanning electron microscopy of specimen faces. The paper studies the appearance, growth, structure, and location of deformation bands, as well as plastic strain in them.

Peer-review under responsibility of the scientific committee of the15th International Conference on Mechanics, Resources and Diagnostics of Materials and Structures.

Keywords: Lüders deformation, profilometer, SEM, digital image correlation method, Chernov–Lüders bands

1. Introduction

In the tensile diagram of the widespread normalized 09G2S steel and its modifications microalloyed with V, Nb, Ti there is a yield plateau indicating the appearance of strain aging Skorokhodov et al. (2011). Herewith, the structure contains fairly large grains, low dislocation density and extremely low content of carbon atoms in ferrite due to the formation of cementite (pearlite) and special carbides, this being suggestive of the action of Lüders deformation having features both similar with the known ones and different from them Khotinov et al. (2019) and Shibkov et al. (2011).

*Corresponding author. +7-950-637-6406
E-mail address: zazma7@mail.ru

Peer-review under responsibility of the scientific committee of the15th International Conference on Mechanics, Resources and Diagnostics of Materials and Structures.
10.1016/j.prostr.2022.04.017

The low yield stress and high plasticity of the normalized 09G2S steel testifies to weak dislocation pinning and low stress concentration during deformation; this manifests itself in a long yield plateau in the tensile diagrams. The low rate of deformation processes offers a matchless opportunity to study them objectively and in detail.

Strain aging is a complex multilevel phenomenon covering all the structural levels of a metal with highly inhomogeneous plastic flow inside and near the deformation bands, in the subsurface regions, in the specimen bulk, etc. This necessitates the simultaneous application of different research methods covering all the levels.

The aim of this paper is to study Lüders deformation (the structure of localized deformation bands and their fronts) by digital image correlation, topography, and scanning electron microscopy of the faces of specimens made of the normalized 09G2S steel.

2. Material and Research Methods

Specimens made of the normalized 09G2S steel (t_A = 950 °C, air cooling), containing (wt%) 0.09 C, 1.28 Mn, 0.35 Si, and 0.17 Cu were studied. The ferrite grain size was 11 μm and the amount of ferrite ranged between 90 and 95%.

Flat specimens sized 3×20×60 mm were tensile tested at the strain rate $\dot{e} = 2.7 \cdot 10^{-4}\ s^{-1}$ in an Instron 8801 machine with the Strain Master optical equipment designed to analyze displacement and strain fields by the digital image (DIC) method.

In order to study the process of the formation of a Chernov–Lüders band CLB in detail, a similar specimen was tested, whose deformation was stopped at the yield plateau with the appearance of a CLB.

The topography of the band surface was studied in a Veeco Wyko NT1100 optical profiling system and a JEOL JSM-6490LV scanning electron microscope.

The simultaneous application of three methods has yielded miscellaneous information on the structure of the band and deformation in it at all the scale levels, namely

- macroscopic (the DIC method with a resolution of ~10^2 μm);
- mesoscopic (topographic studies with a resolution of ~10 μm);
- microscopic (scanning electron microscopy with a resolution of ~$5 \cdot 10^{-2}$ μm).

3. Experiment Results and Discussion

In the stress-strain diagram there are a pronounced sharp yield point and a clear yield plateau (Fig. 1), which testify to the manifestation of the effect of strain hardening. Characteristic points 1 to 5 are highlighted in the diagram within the yield plateau.

The band nucleus is formed at the stage of pre-yielding near the lateral face of the specimen. The region around the dipole peak, from which a deformation band grows (Fig. 2), is here referred to as the nucleation center (NC). According to the white spot (point 4 in Fig. 2a), the maximum value of ε_{yy} is reached in the NC; the CLB exiting from it is first perpendicular to the edge, and then arranged at an angle of 60° to it.

The dislocations exiting from the initial NC_i and forming a CLB belong to the main slip system (a/2<111>{110} for ferrite) and spread along the directions of maximum tangential stresses. Consequently, the primary sources of dislocations moving in the band lie on the surface of the NC_i; under specimen tension, as the NC_i grows in size, the number of such dislocation sources increases, and this results in band broadening (transverse growth) through the appearance of new microbands inside the CLB.

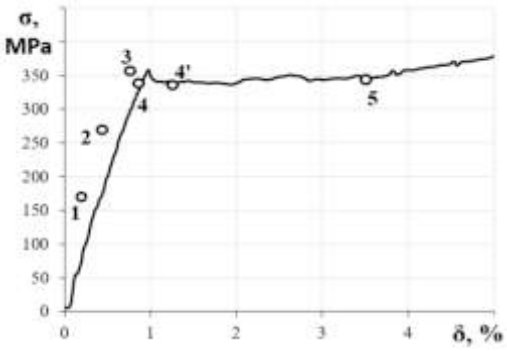

Fig. 1. The initial portion of the tensile diagram for a 09G2S steel specimen.

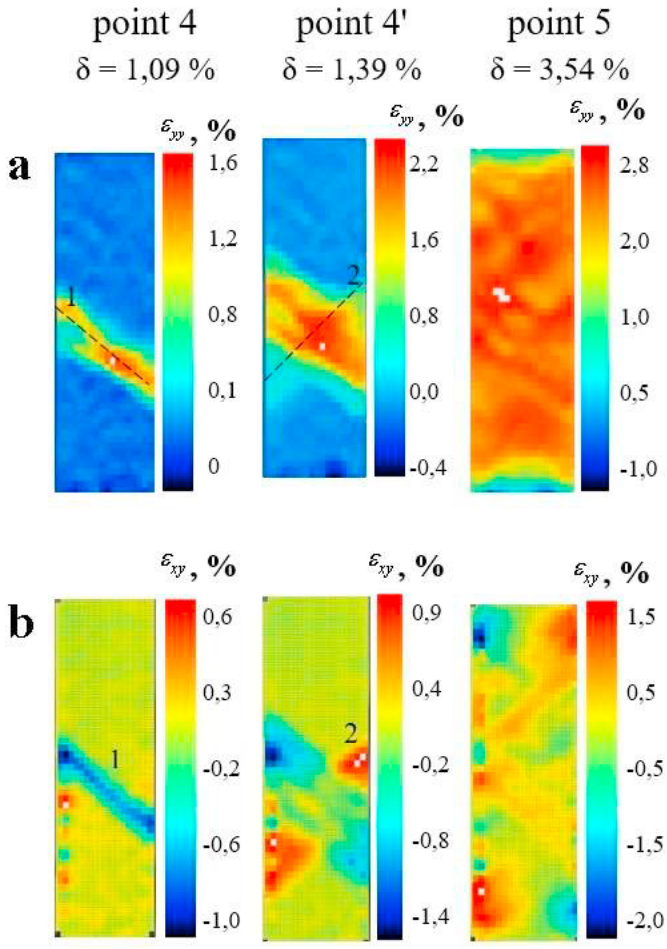

Fig. 2. Strain field patterns in a 09G2S steel specimen: longitudinal ε_{yy} (a) and shearing ε_{xy} (b).

The size and shape of the region of band nucleus entrance into the opposite edge are close to those of the NC_i. This enables us to call this region the nucleation center of the band end NC_e and in many cases to study the similar behavior of these regions.

The arrangement of the deformation bands can be explained in geometric terms. Firstly, the distance between the nucleation centers is equal to the length of the standing wave λ since the nucleation centers are formed from dipole peaks, i.e. standing elastic wave peaks Farber et al. (2019). This specifies the number of nucleation centers on each edge as $n = L_{sp}/\lambda = 4$, where L_{sp} is the length of the gauge of the specimen. Secondly, since primary a/2<110>{111} dislocations spread in the bands, the latter are arranged at an angle of 60° to the edges, i.e. to the specimen tensile axis. Particularly, the angle between the <110> planes is 60°.

On the maps of ε_{xy}, where ε_{xy} bands 1 and 2, different in sign, are differently colored, there is a band intersection region (Fig. 2b) even at the beginning of the yield plateau (point 4 in the σ–δ diagram). At the intersection of conjugate bands 1 and 2 there is a deformation site, always colored red on ε_{yy} maps since all the bands have a positive longitudinal component ε_{yy} of the strain tensor (Fig. 2a).

The analysis of the profiles of ε_{yy} distribution along the path passing through the specimen middle, parallel to the loading axis P, has shown that the increase in δ under tension on the yield plateau leads to an increase in ε_{yy}^{max} and band broadening through the entire profile, i.e. to plastic strain accumulation in the band at the rate $\Delta S/\Delta\tau = 16.74\%/s$ ($\Delta S/\Delta\delta = 23.81$), where S is the area under the ε_{yy}–L_{sp} curve, the grad ($\Delta\varepsilon_{yy}/\Delta L_{sp}$) over a large portion of the ε_{yy}–L_{sp} curves being constant. The CLB width including the major peak of ε_{xy} and two minor ones is equal to the width of the peak of ε_{yy} (L_w^{yy}= 15 mm); consequently, the minor peaks of ε_{xy} belong to the band.

Thus, starting from the first moments of band formation, band broadening (transverse growth) is accompanied by plastic flow in the band. This entails the conclusion that the appearance, motion, and accumulation of dislocations in the band, as well as the sink of dislocations and vacancies from the band center to its periphery, cause the motion of the fronts.

Due to better resolution, the topographic method reveals the details of the CLB structure that fail to be revealed by the DIC method, namely first of all inhomogeneity over the length, width, and depth of the band.

Plastic flow in the band arranged at an angle of ~60° to the tensile axis forms a green hollow with the depth $h \approx (10…30)$ μm (I in Fig. 3). On both sides it is surrounded by elevations of a variable color up to red, which obviously look as minor peaks on the ε_{xy}–L_{sp} profiles. In a considerable length near the tensile axis the band has a trapezoidal shape with a wide side on the front surface of the specimen, oblique fronts going deep inside, and a narrow flat bottom. The widest (~25 μm) and deepest regions near the specimen edges (A and B in Fig. 3) seem to be nucleation centers (NC) with the maximum ε_{yy} component, which can be found on the DIC maps (Fig. 2).

The analysis of CLB evolution has shown that the formation of the deformation band is associated with the simultaneous action of two plastic flow mechanisms:

- band-type, responsible mainly for the longitudinal growth of the band – with the motion of dislocations of the main slip system;
- not concentrated in one plane – with the lateral growth (broadening) of the CLB along the tensile axis by e.g., double transverse slip or activation of new dislocation sources from stress concentration in the undeformed regions adjacent to the band Shtremel (1997).

At the sites of band exit onto the specimen sides there appears a microscopic neck (→ in Fig. 3) slanting to the tensile axis. The transverse strain component in the middle of the microscopic neck relative to the initial specimen width is

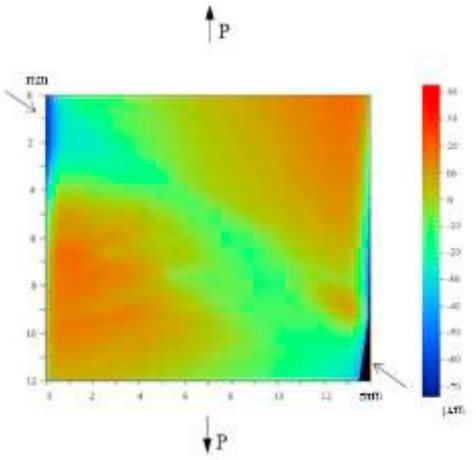

Fig. 3. Chernov–Lüders band topogram.

$$\varepsilon=(B_0-B_i)/B_0\cdot 100\%\approx 14\% \quad (1)$$

where B_0 and B_i are the initial specimen width and that in the middle of the microneck, respectively. In the band outlet (region A in Fig. 3) the strain reaches 20%. This agrees with the data obtained by other procedures in Farber et al. (2020) and suggests the formation of a cellular dislocation structure in the deformed ferrite Shtremel (1997) and Honeycomb (1984).

CLB regions I and II (Fig. 3) were studied by SEM, and they demonstrated identical structures (Fig. 4). As in Farber et al. (2020), it has been found that the macroband consists of parallel microbands with a width of 17 to 20 μm. The microbands with the finest structure are surrounded by microbands with coarser structural elements. Judging by the fragmentation and oblongness of the nonmetallic inclusion particles, probably MnS, the microbands have suffered significant plastic deformation, which has formed rounded fragments with a diameter of 0.3 to 0.5 mm, with orientation gradually changing inside and abruptly changing at the microband boundaries (Fig. 4b). Proceeding from a considerable value of local strain in the band ($\varepsilon \approx 14\%$), increased microhardness, and a change of the texture components (EBSD), one can suppose that these fragments are dislocation cells. In the regions with the fragments (cells) perpendicular to the specimen surface under study it is obvious that they are ~0.015 μm thick close parallel thin disks, sometimes curved (↑ in Fig. 4a).

Translational-rotational plastic flow is the main mechanism of metal deformation Shtremel (1997). It means that lattice shear accompanied by the accumulation of excess similar dislocations on the surface of structural elements (dislocation cell walls, microscopic and macroscopic bands, deformation zone front) results in dislocation rotation relative to the surrounding volumes.

This can be observed from the rapid increase of the ε_{xy} component associated with rotation in the nucleation centers and consequently in bands 1 and 2 before intersection.

The joint rotation of cells in the band, which is governed by the dislocations of the primary slip system, creates natural rotation (first elastic and then plastic) of the growing band relative to the surrounding volume, where the initial dislocation density remains unchanged. The ε_{yy} and ε_{xy} profiles testify that the maximum strain (dislocation density) occurs in the middle of the band and that it decreases with a considerable gradient towards the band periphery, or fronts.

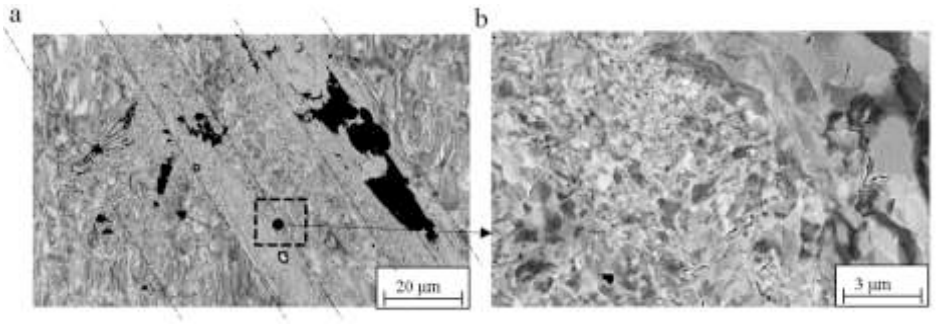

Fig. 4. SEM images of a Chernov–Lüders band.

The staggered dipole arrangement of the nucleation centers of bands 1 and 2 testifies to the rotation of the "upper" and "lower" parts of the deformation site to different sides. Subsequently, the remaining parts of the specimen, i.e., external deformation sites, are involved in the rotation. The appearance of external bands with a certain sign of ε_{xy} specifies the same rotation direction of the external deformation sites as that of the "upper" and "lower' parts of the primary deformation sites that contact them.

The image of the bands in the intersection region gradually disappears, and there appear yellow fragments instead, which are separated by green areas with the value of ε_{xy} close to 0% (point 5 in Fig. 2b).

The suppression of ε_{xy} at the band intersection should be viewed as rotation neutralization of rotation inside the bands due to almost complete suppression of the rotational component of the deformation of dislocation cells. In bands 1 and 2 the rotation of dislocation cells, which is caused by excess dislocations of the primary slip system in their walls, occurs in different directions, this being depicted by different band colors on the ε_{xy} maps. We assume that, in the intersection region, dislocations of different slip systems of the main family interact in the walls. This forms differently directed torques, whose resultant action (M_Σ) is determined as $M_\Sigma = M_1 - M_2$, i.e. by the difference in the density ρ_d of dislocations entering the intersection region from bands 1 and 2; $M_\Sigma = 0$ when $\rho_d^{B1} \approx \rho^{B2}$.

The band intersection regions in the middle of the specimen and in the nucleation centers, where the value of ε_{xy} is minimum and close to zero, have the largest ε_{yy} component at the i-th moment of tension (white spots on the ε_{yy} maps shown in Fig. 2a). Consequently, under conditions of constrained deformation, minimization of expenditure for the rotation of the structure elements drastically facilitates the translational component of plastic flow. Easy shearing is also promoted by the increased dislocation mobility inside the cells where there occurs the increased concentration of vacancies at the intersection of dislocations belonging to conjugate bands.

4. Conclusion

Investigation by the methods of digital image correlation, topography, and scanning electron microscopy has revealed that Chernov–Lüders bands in the 09G2S steel suffer considerable plastic strain ε (up to ~14%), and this causes ferrite and pearlite grain refinement and elongation along the band direction.

It has been found that the Chernov–Lüders band consists of a group of 17…20 μm wide parallel microbands containing rounded fragments, different in size (from 0.3…0.5 to 3…7 μm) and orientation.

In the deformation site, starting from the regions of intersection of conjugate bands, suppression of the ε_{xy} component down to zero has been detected, which is accompanied by the maximum value of the ε_{yy} component. This is considered to result from the neutralization of the rotational strain component due to the attenuation of the rotation of dislocation cells, which facilitates the action of the translational component of plastic flow.

Acknowledgements

The study was performed at the IMP UB RAS under a state assignment from the Ministry of Education and Science of Russia (theme Structure, No. AAAA-A18-118020190116-6) and within the research plan of the IES UB

RAS (theme No. AAAA-A18-118020790145-0). The equipment of the shared access center (Yeltsin UrFU) and the Plastometriya shared access center (IES UB RAS) was used in the testing.

References

Farber V.M., Polukhina O.N., Vichuzhanin D.I., Khotinov V.A., Smirnov S.V., 2019. A study of plastic deformation of 08G2B steel before and at the yield plateau by digital image correlation technique. Part 1. Formation of plastic and elastic deformation waves. Material Science and Heat Treatment 61, 274–279.

Farber V. M., Morozova A. N., Khotinov V. A., Karabanalov M. S., Schapov G. V, 2020. Plastic Flow in a Chernov–Luders Band in Ultrafine-Grained 08G2B Steel. Physical Mesomechanics 23, 340—346.

Honeycomb R.W.K. 1984. The Plastic Deformation of Metals. 2nd ed. E. Arnold Publ., London, pp. 483.

Khotinov V.A., Polukhina O.N., Vichuzhanin D.I., Schapov G.V., Farber V.M., 2019. Study of Luders deformation in ultrafine low-carbon steel by the digital image correlation technique. Letters of Materials 9(3), 328-333.

Skorokhodov V.N., Odessky P.D., Rudchenko A.V., 2002. Building Steel. Metallurgiya, Moscow, pp. 624.

Shibkov A.A., Zolotov A.E., Zheltov M.A., Denisov A.A., 2011. Morphological transition from the Euclidean to the fractal shape of the Lüders band in the aluminum-magnesium alloy AMg6. Physics of the Solid State 3(5), 887–895.

Shtremel M.A. 1997 Strength of Alloys. Part 2. Deformation. MISiS, Moscow, pp. 527.